analytical chemistry

Article

pubs.acs.org/ac

Electrogenerated Chemiluminescence Resonance Energy Transfer between $Ru(bpy)_3^{2+}$ Electrogenerated Chemiluminescence and Gold Nanoparticles/Graphene Oxide Nanocomposites with Graphene Oxide as Coreactant and Its Sensing Application

Yong-Ping Dong,[†,‡] Ying Zhou,[†,‡] Jiao Wang,[†,‡] and Jun-Jie Zhu*[,†]

[†]State Key Laboratory of Analytical Chemistry for Life Science, School of Chemistry and Chemical Engineering, Nanjing University, Nanjing 210093, China

[‡]School of Chemistry and Chemical Engineering, Anhui University of Technology, Maanshan 243002, China

Supporting Information

ABSTRACT: In the present work, strong anodic electrogenerated chemiluminescence (ECL) of $Ru(bpy)_3^{2+}$ was observed at a graphene oxide modified glassy carbon electrode (GO/GCE) in the absence of coreactants. The electrocatalytical effect of GO on the oxidation of $Ru(bpy)_3^{2+}$ suggested that GO itself can act as the coreactant of $Ru(bpy)_3^{2+}$ ECL, which can be used to fabricate the ECL biosensor. Thiol group terminated adenosine triphosphate (ATP) aptamer was immobilized on the GO film via DNA hybridization. When gold nanoparticles/graphene oxide (AuNPs/GO) nanocomposites were modified on the aptamer through the S−Au bond to form a sandwich-like structure, the ECL resonance energy transfer (ECL-RET) could occur between $Ru(bpy)_3^{2+}$ and AuNPs/GO nanocomposites, resulting in an apparent decrease of ECL signal. After the ECL sensor was incubated in ATP solution, the AuNPs/GO nanocomposites were released from the electrode due to the specific interaction between aptamer and ATP, leading to the increased ECL signal. On the basis of these results, an ECL aptasensor was fabricated and could be used in the sensitive and selective detection of ATP in the range of 0.02−200 pM with a detection limit of 6.7 fM (S/N = 3). The proposed ECL aptasensor can be applied in the detection of ATP in real samples with satisfactory results.

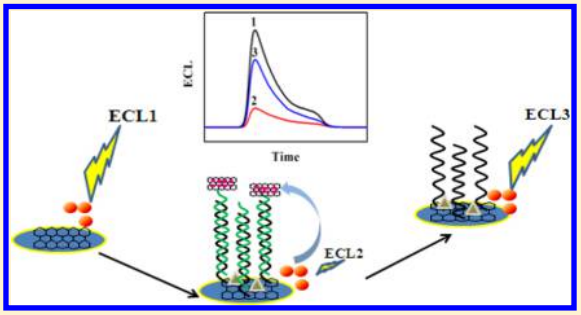

It is well-known that electrogenerated chemiluminescence (ECL) has potential advantages over other analytical methods, and several commercial ECL systems have already been used in clinical detection.[1,2] Luminol, quantum dots, and Ru complexes are the most famous ECL systems in the fabrication of ECL biosensors.[3−5] Among these ECL systems, tris(2,2′-bipyridyl) ruthenium(II) ($Ru(bpy)_3^{2+}$) and its derivatives have been intensively studied due to their outstanding properties.[6,7] Coreactants are often needed to obtain strong $Ru(bpy)_3^{2+}$ ECL, and numerous coreactants have been investigated in the past few decades, including oxalate, alkylamines, NADH, amino acids, dopamine, and ascorbic acid.[8−15] These work revealed that $Ru(bpy)_3^{2+}$ ECL depended significantly on the properties and structures of coreactants. Therefore, the exploration of a new coreactant of $Ru(bpy)_3^{2+}$ ECL is necessary for its application in bioassay.

Recently, luminescence resonance energy transfer (LRET) has attracted much research interest as a powerful technique for the sensitive detection of biomolecules. Three kinds of LRET have often been reported in bioassays, including fluorescence resonance energy transfer, chemiluminescence resonance energy transfer, and bioluminescence resonance energy transfer.[16−21] As another highly sensitive luminescent technique, however, ECL resonance energy transfer (ECL-RET) has been paid rare attention to for the lack of suitable energy donor/acceptor pairs.[21] Consequently, the exploration of more energy donor/acceptor pairs is urgent for ECL-RET investigation.

Because of high surface area and high $\pi-\pi$ conjunction, graphene oxide (GO) can provide a platform for the immobilization of organic and inorganic molecules, which promotes the development of graphene oxide based ECL sensors.[22,23] For example, GO can immobilize tris(1,10-phenanthroline) ruthenium to fabricate ECL biosensor for highly sensitive detection of methyltransferase activity.[24] When CdSe quantum dots were immobilized on graphene oxide/polyaniline nanowires composite, its ECL signal was enhanced greatly, which can be used to fabricate ECL immunosensor for the detection of human interleukin-6.[25] GO can also be used to immobilize DNA using carbodiimide chemistry, and from the combination of graphene-like nanomaterials with aptamers has emerged many ingenious aptasensing strategies for the applications in clinical diagnosis.[26,27] Except its excellent

Received: March 8, 2016
Accepted: April 21, 2016
Published: April 21, 2016

DOI: 10.1021/acs.analchem.6b00921
Anal. Chem. 2016, 88, 5469−5475

application in electrode modification, GO has the photoluminescence arising from electron−hole pairs, and water-soluble GO can generate ECL with $S_2O_8^{2-}$ as coreactant.[28−31] Recently, Seo and co-workers have demonstrated that GO photoluminescence could be quenched by gold nanoparticles (AuNPs) because of fluorescence resonance energy transfer between GO and AuNPs.[26,32] Resonance energy transfer was also obtained between reduced graphene-AuNPs and CdTe quantum dots.[33] These work revealed that GO and AuNPs are suitable materials for the ECL-RET research, which has not been reported previously.

In this work, strong anodic ECL of $Ru(bpy)_3^{2+}$ was obtained at the GO modified GCE (GO/GCE) in the neutral condition without coreactant. Amino terminated DNA was immobilized on the GO film through the amidation between $-NH_2$ and carboxyl groups of GO. Then, thiol terminated adenosine triphosphate (ATP) aptamer was connected through DNA hybridization. When AuNPs/GO nanocomposites were assembled on the aptamer through the interaction between AuNPs and thiol groups, a sandwich-like structure was formed. ECL-RET could occur between $Ru(bpy)_3^{2+}$ and AuNPs/GO composites, leading to the decrease of ECL signal. The specific interaction between ATP and aptamer could destroy the sandwich-like structure and release AuNPs/GO nanocomposites from the modified electrode, resulting in the increased ECL signal again, which varied linearly with ATP concentrations. As a result, an ECL aptasensor for ATP detection was proposed.

EXPERIMENTAL SECTION

Materials and Reagents. Graphite (99.95%, 8000 mesh) was obtained from Aladdin Industrial Corporation. Tris(2,2′-bipyridyl) ruthenium(II) dichloride hexahydrate ($Ru(bpy)_3Cl_2 \cdot 6H_2O$), poly(diallyldimethylammonium chloride) (PDDA, 20% w/w in water, MW = 200 000−350 000), adenosine triphosphate (ATP), cytidine triphosphate (CTP), guanosine triphosphate (GTP), uridine triphosphate (UTP) were purchased from Aladdin Chemistry Co., Ltd. Human serum was obtained from Nanjing Military Region General Hospital (Nanjing, China). Tris(2-carboxyethyl)phosphine (TCEP), bovine serum albumin (BSA), 1-ethyl-3-(3-(dimethylamino) propyl) carbodiimide hydrochloride (EDC), and *N*-hydroxysuccinimide (NHS) were purchased from Sigma-Aldrich. Chloroauric acid ($HAuCl_4 \cdot 4H_2O$) was obtained from Shanghai Reagent Company (Shanghai, China). All other chemicals were of analytical reagent grade, and double distilled water was used throughout. The 0.1 mol L^{-1} pH 7.4 phosphate buffer solution (PBS) was used to prepare the working solution for ECL detection. Tris-HCl buffer solution (pH 7.4, 10 mM) containing 0.1 mol L^{-1} NaCl was adopted to prepare DNA stock solutions.

The 30-mer ATP binding aptamer (S2) and its complementary strand DNA (S1) were synthesized and purified by Shanghai Sangon Biological Engineering Technology & Service Co., Ltd. (Shanghai, China). The sequences used are as follows:

DNA (S1): 5′-NH_2-$(CH_2)_6$-ACC TTC CTC CGC AAT ACT CCC CCA GGT-3′

Aptamer (S2): 5′-SH-$(CH_2)_6$-*ACC TGG GGG AGT ATT GCG GAG GAA GGT* CAG-3′

(The italicized part is the complementary strand of the ATP binding aptamer.)

Synthesis of AuNPs. AuNPs were synthesized according to the reported method with some modifications.[34] Briefly, an aqueous solution containing 75 mL of double distilled water, 1.5 mL of 25 mM $HAuCl_4$, and 5 mL of 10 mM trisodium citrate was first prepared in a conical flask. Next, 1.5 mL of ice-cold, freshly prepared 0.1 mol L^{-1} $NaBH_4$ solution was added into the above solution while stirring. The mixture solution turned pink immediately after adding $NaBH_4$, indicating nanoparticles formation. After stirring for 6 h at room temperature, the resulting AuNPs solution was obtained and kept at 4 °C for further use. The morphologies of AuNPs were characterized by TEM.

Preparation of AuNPs/GO Nanocomposites and S2/AuNPs/GO Probe. Graphene oxide (GO) and AuNPs/GO nanocomposites were synthesized according to the previous reports.[35−37] The AuNPs/GO nanocomposites were resuspended in 1 mL of PBS containing 100 nM aptamer (S2), which was activated with 10 mM tris(2-carboxyethyl)phosphine and stirred for 12 h at room temperature. Excess amount of AuNPs/GO nanocomposites was removed by centrifugation with 10 000 rpm at 4 °C for 30 min. The supernatant containing S2/AuNPs/GO was decanted and stored at 4 °C prior to the electrode modification.

Fabrication of ECL Aptasensor. Prior to the sensor fabrication, glassy carbon electrode (GCE, 3 mm in diameter) was polished to a mirror using 1.0 and 0.05 μm alumina slurry followed by sonication in water and ethanol, respectively. The cleaned electrode was dried at room temperature. Then, 10 μL of GO suspension was spread on the surface of cleaned GCE. After the GO film was dried in the air, the carboxylic groups on the GO film were activated in 10 mM EDC and 20 mM NHS solutions for 0.5 h. After the electrode was washed with PBS (pH 7.4), 10.0 μL of S1 (100 nM) was dropped onto its surface to incubate at 4 °C for 12 h. Then, the modified electrode was washed thoroughly with PBS to remove the unlinked S1 and was immersed into 1% BSA solution for 1 h to block the nonspecific binding sites. Afterward, 10 μL of S2/AuNPs/GO was dropped onto the S1 modified electrode to incubate at 37 °C for 1 h. The excess amount of S2/AuNPs/GO was washed with PBS.

ECL Detection. ECL signal was recorded in 0.1 mol L^{-1} pH 7.4 PBS containing 66 μM $Ru(bpy)_3^{2+}$ with the modified electrode as the working electrode. For the detection of ATP, the prepared modified electrode was incubated in different concentrations of ATP for 90 min at 37 °C, followed by thoroughly washing with PBS to remove the unbound ATP and the disassembled aptamer-ATP conjugate. Human serum samples were diluted with pH 7.4 PBS to a suitable concentration for ATP detection. The practical samples were spiked with various concentrations of ATP and detected using the above method.

RESULTS AND DISCUSSION

Electrochemical and ECL of $Ru(bpy)_3^{2+}$ at the GO/GCE. GO has already been used in ECL investigation. For example, GO could inhibit luminol ECL while electrochemical reduced GO could enhance luminol ECL.[38] GO was used as the matrix for the immobilization of $Ru(phen)_3^{2+}$ through the π−π stacking interaction and the electrostatic interaction, and strong ECL could be obtained with tripropylamine as coreactant.[39] However, $Ru(bpy)_3^{2+}$ ECL at the GO modified electrode in the absence of coreactant has never been reported. Herein, the ECL of $Ru(bpy)_3^{2+}$ is studied at the GO/GCE in neutral PBS under air-saturated conditions without coreactant. The anodic ECL at the bare GCE is extremely weak in the absence of

DOI: 10.1021/acs.analchem.6b00921
Anal. Chem. 2016, 88, 5469−5475

coreactant (Figure 1). No ECL signal is observed at the GO/GCE in PBS, suggesting that GO cannot emit light under this

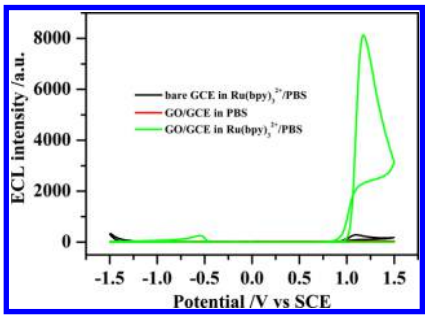

Figure 1. ECL curves of the GO/GCE in 0.1 mol L^{-1} PBS and the bare GCE and the GO/GCE in 0.1 mol L^{-1} PBS containing 66 μM $Ru(bpy)_3^{2+}$. Potential scan rate, 100 mV s^{-1}; pH, 7.4.

condition. In the presence of $Ru(bpy)_3^{2+}$, one strong anodic ECL peak can be obtained at 1.17 V, which is 32-times larger than that of the bare GCE. The weak ECL peak at −0.55 V is related to the oxygenated groups of graphene oxide, because this peak cannot be obtained when the GO film was electrochemically reduced and the ECL intensity does not change with $Ru(bpy)_3^{2+}$ concentration. The strong anodic ECL at the GO/GCE reveals that GO can act as a coreactant in ECL reaction of $Ru(bpy)_3^{2+}$, which can be used in bioassays.

In order to elucidate the mechanism of anodic ECL at the GO/GCE, the cyclic voltammograms of $Ru(bpy)_3^{2+}$ at the bare GCE and the GO/GCE were recorded as shown in Figure 2. At

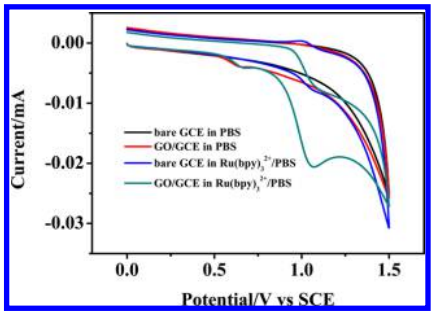

Figure 2. Cyclic voltammograms of bare GCE and GO/GCE in $Ru(bpy)_3^{2+}$/PBS. PBS, 0.1 mol L^{-1}; $Ru(bpy)_3^{2+}$, 66 μM; pH, 7.4; scan rate, 100 mV s^{-1}.

the bare GCE, a pair of reversible redox peaks at 1.10 V can be attributed to the oxidation−reduction of $Ru(bpy)_3^{2+}$. At the GO/GCE, the oxidation potential of $Ru(bpy)_3^{2+}$ is negatively shifted to 1.06 V and the oxidation current increases 3-times compared with the bare GCE, suggesting that the oxidation of $Ru(bpy)_3^{2+}$ is catalyzed by GO. The reduction peak of $Ru(bpy)_3^{2+}$ almost disappears, revealing that the oxidation product of $Ru(bpy)_3^{2+}$ ($Ru(bpy)_3^{3+}$) is consumed before its electrochemical reduction. Bard et al. reported that $Ru(bpy)_3^{3+}$ could react with TPA to generate TPA radicals, which resulted in the decrease of reduction current of $Ru(bpy)_3^{2+}$.[40] Therefore, it can be concluded that $Ru(bpy)_3^{3+}$ can react with GO before its electrochemical reduction. The weak oxidation peak at 0.65 V observed in PBS with and without $Ru(bpy)_3^{2+}$ can be assigned to the oxidation of H_2O to $OH^{\bullet}$.[41]

It was proposed that carboxylic acid can be oxidized by electrogenerated $OH^{\bullet}$ to form the strong reducing intermediates $CO_2^{\bullet-}$ which could act as a coreactant and react with $Ru(bpy)_3^{3+}$ to emit light.[42] It has already been confirmed that carboxyl group and other oxygenated groups can be found on the GO sheet.[38] The anodic ECL decreased greatly when GO film was electrochemically reduced at −1.0 V for 20 min, revealing that oxygenated groups are necessary for the anodic ECL (Figure S1). The ECL intensity decreased under N_2-saturated condition compared with air-saturated condition also supported the above conclusion. The ECL spectrum suggested that the light emitter of the anodic ECL peak should be the excited state of $Ru(bpy)_3^{2+}$ (Figure S2). Therefore, the mechanisms of anodic $Ru(bpy)_3^{2+}$ ECL at the GO/GCE should be as follows:

$$H_2O - e^- \rightarrow H^+ + OH^{\bullet} \quad (1)$$

$$GO{-}COOH + OH^{\bullet} \rightarrow GO{-}CO_2^{-\bullet} + H_2O \quad (2)$$

$$Ru(bpy)_3^{2+} - e^- \rightarrow Ru(bpy)_3^{3+} \quad (3)$$

$$GO{-}CO_2^{-\bullet} + Ru(bpy)_3^{3+} \rightarrow Ru(bpy)_3^{2+*} \rightarrow Ru(bpy)_3^{2+} + h\nu \quad (4)$$

Characterization of AuNPs/GO Nanocomposites. It was reported that the fluorescence resonance energy transfer can occur between the reduced graphene oxide/AuNPs and CdTe quantum dots due to the overlap of absorption and emission spectra.[33] Spurred by these results, AuNPs/GO nanocomposites were synthesized and tentatively used to fabricate the ECL-RET system in the present work. The morphologies of GO, AuNPs, and AuNPs/GO nanocomposites were characterized by transmission electron microscopy (TEM), scanning electron microscopy (SEM), and Raman spectroscopy as shown in Figure 3.

It can be found that GO exhibits a typically wrinkled, sheet-like structure with no aggregation (Figure 3A). In the Raman spectra of GO, the D band and G band located at 1359 and 1600 cm^{-1} can confirm the structure of GO (Figure 3B).[43] The average size of AuNPs is estimated to be 6 nm according to the

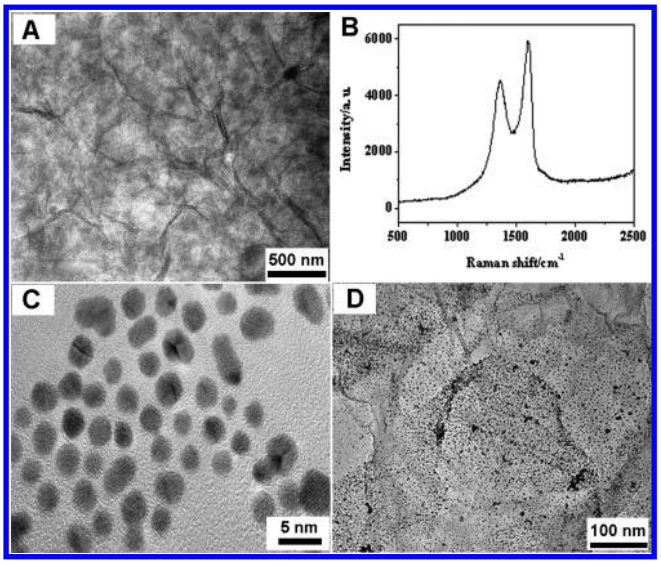

Figure 3. (A) SEM image of GO, (B) Raman spectrum of GO, (C) TEM image of AuNPs, and (D) SEM image of AuNPs/GO.

DOI: 10.1021/acs.analchem.6b00921
Anal. Chem. 2016, 88, 5469−5475

Scheme 1. Schematic Representation of the Modification of the GCE and the Detection of ATP

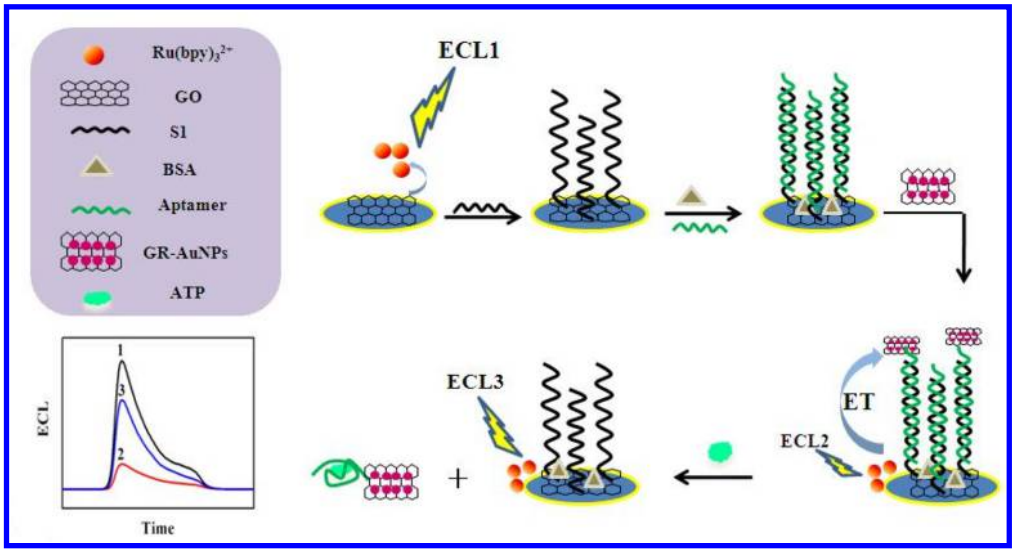

TEM image in Figure 3C. Larger sizes of AuNPs, including 16 and 38 nm, were also used in the energy transfer investigation, and no apparent resonance energy transfer was observed. Therefore, 6 nm of AuNPs was selected. The SEM image of AuNPs/GO nanocomposites exhibits a homogeneously dispersion (Figure 3D). The UV−vis absorption spectrum of the nanocomposite was recorded as shown in Figure S3. Because the absorption spectrum of nanocomposite overlaps with the emission spectrum of $Ru(bpy)_3^{2+}$, resonance energy transfer can occur between them.

Fabrication and Characterization of ECL Aptasensor. Nucleic acid aptamers are single-stranded DNA or RNA oligonucleotides with high affinity and specificity toward their targets. Various aptamer-based biosensors have been developed using the specific identification of aptamer toward their target. Herein, an ECL aptasensor involving ATP binding aptamer and AuNPs/GO nanocomposite is proposed for the detection of ATP as shown in Scheme 1.

GO was modified on the bare GCE to generate strong anodic ECL with $Ru(bpy)_3^{2+}$ in the absence of ATP. The ATP aptamer and AuNPs/GO nanocomposite were assembled on the electrode in sequence through DNA hybridization to form sandwich-like structure, leading to the decreased ECL signal due to the energy transfer (ET) between $Ru(bpy)_3^{2+}$ and AuNPs/GO nanocomposites. When ATP was bonded to its aptamer, the sandwich-like structure was destroyed, and AuNPs/GO nanocomposites were released from the modified electrode, resulting in the increased ECL again. As a result, an ECL aptasensor was fabricated and can be used to detect ATP.

The fabrication processes of the ECL aptasensor were confirmed by recording ECL signals in different assembly stages as shown in Figure 4. The GO/GCE showed a greatly enhanced ECL signal at 1.2 V in air-saturated pH 7.4 PBS containing 66 μM $Ru(bpy)_3^{2+}$. After S1 was bonded onto the GO/GCE, the ECL intensity decreased due to the insulating property of DNA. The ECL intensity further decreased when S1 was bonded with ATP aptamer (S2). When AuNPs were connected on the aptamer, ECL intensity decreased due to the resonance energy transfer between AuNPs and $Ru(bpy)_3^{2+}$.[33] After AuNPs/GO was connected on the aptamer to form the sandwich-like structure, ECL intensity was further weakened, revealing that the resonance energy transfer can be improved in

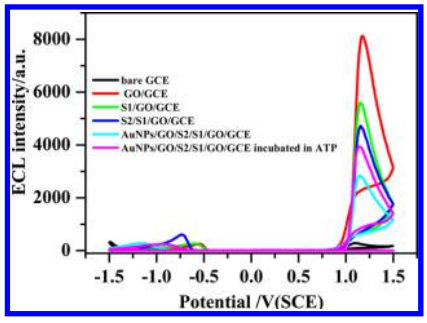

Figure 4. ECL profiles of different modified electrodes in 66 μM $Ru(bpy)_3^{2+}$ and 0.1 mol L^{-1} PBS. Potential scan rate, 100 mV s^{-1}; pH, 7.4.

the presence of GO (Figure S4). Therefore, AuNPs/GO and $Ru(bpy)_3^{2+}$ was selected as the energy donor/acceptor pair for ECL-RET. When the aptasenor was incubated in 1 pM ATP, the sandwich-like structure was destroyed and the ECL signal increased again.

Electrochemical impedance spectroscopy (EIS) is often used to characterize the surface properties of the modified electrodes during the biosensor fabrication process. It can be found from Figure 5 that the Nyquist diagrams of all electrodes consisted of a semicircle at high frequency and a line at low frequency. The

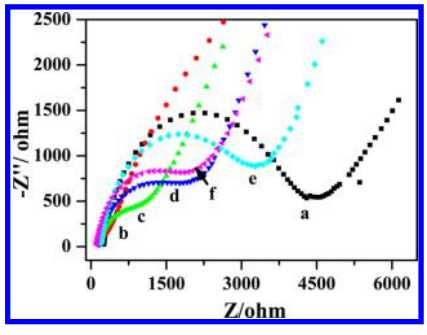

Figure 5. Electrochemical impedance spectroscopy of bare GCE (a), GO/GCE (b), S1/GO/GCE (c), S2/S1/GO/GCE (d), AuNPs/GO/S2/S1/GO/GCE (e), and AuNPs/GO/S2/S1/GO/GCE incubated in 1 pM ATP (f).

DOI: 10.1021/acs.analchem.6b00921
Anal. Chem. 2016, 88, 5469−5475

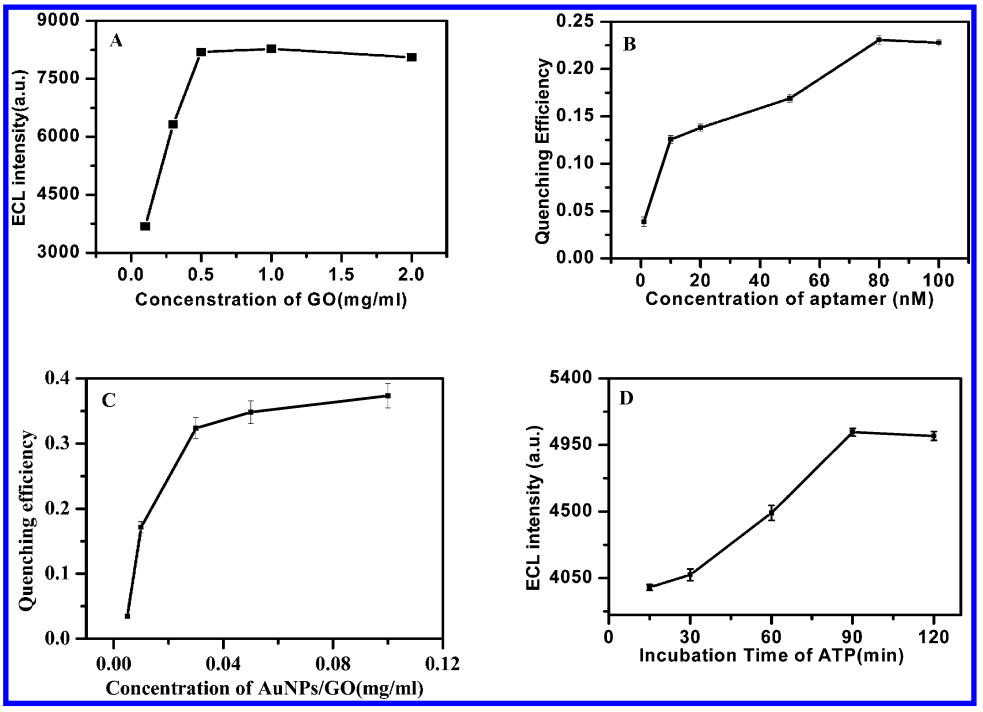

Figure 6. (A) Effects of GO concentration on ECL signals. (B) Effect of aptamer concentration on ECL signals. (C) Quenching effect of AuNPs/GO on ECL signals. (D) Effect of the incubation time in 50 pM ATP on ECL intensity.

charge transfer resistance (R_{ct}), which equals the diameter of the semicircle, reflects the restricted diffusion of the redox probe through the multilayer system. The EIS of the bare GCE exhibited a semicircle with a large diameter at high frequency. The EIS of the GO/GCE is nearly a line in all of the frequency range, suggesting that R_{ct} of the GO/GCE decreased significantly compared with the bare GCE, which could be attributed to the good conductivity of GO. After EDC/NHS activation, S1 was bonded on the GO film through the interaction between amine and carboxyl groups, leading to an increase of R_{ct} due to the poor conductivity of single strand DNA.[33] After the electrode was incubated in S2/AuNPs/GO, the R_{ct} increased due to the electrostatic repulsion between the negatively charged S2/AuNPs/GO and $[Fe(CN)_6]^{3-/4-}$ probe, indicating the successful hybridization of S2/AuNPs/GO. The results of zeta potential also support the above conclusions (Figure S5). The R_{ct} diminished after the introduction of ATP, which could be attributed to the partial destruction of the sandwich-like structure. The EIS results confirmed the successful stepwise fabrication of the proposed ECL aptasensor.

Optimization of Detection Conditions. Since GO can act as the coreactant of $Ru(bpy)_3^{2+}$ ECL, the anodic ECL intensity should depend on the concentration of GO suspension. As shown in Figure 6A, the ECL intensity of the modified electrode increased with the increase of GO concentration and reached a plateau at 0.5 mg/mL. To obtain high ECL intensity, 0.5 mg/mL GO suspension was chosen to modify the electrode. The effect of $Ru(bpy)_3^{2+}$ concentration on ECL was also studied as shown in Figure S6. The ECL signals increased with the increase of $Ru(bpy)_3^{2+}$ concentration. Considering the detection sensitivity and the reduction of the consumption of luminescent reagents, 66 μM $Ru(bpy)_3^{2+}$ was selected.

It can be concluded from the assembly strategy of the aptasensor that the aptamer (S2) can bond AuNPs/GO to form sandwich-like structure, resulting in the decreased ECL intensity due to the ECL-RET. Therefore, the effect of aptamer concentration on the ECL intensity was examined as shown in Figure 6B. It can be found that the quenching efficiency (quenching efficiency = I/I_0, where I was the ECL signals after S2/AuNPs/GO was connected on S1 and I_0 was the ECL signals before S2/AuNPs/GO was connected on S1) gradually increased with the increase of aptamer concentration, and a plateau can be obtained when aptamer concentration reached 80 nM, indicating a saturated capture of aptamer. As a result, 10.0 μL of 80 nM aptamer was selected.

Because AuNPs/GO nanocomposites are the energy acceptor in ECL-RET, the concentration of AuNPs/GO nanocomposites aqueous suspension can influence energy transfer processes. It can be found from Figure 6C that more AuNPs/GO was captured by the aptasensor with the increase of the AuNPs/GO suspension concentration, and the quenching efficiency increased correspondingly. In order to obtain ideal quenching efficiency, 0.05 mg/mL AuNPs/GO suspension was chosen.

The incubation times of the modified electrode in 50 pM ATP solution were optimized as shown in Figure 6D. With the increase of the incubation time in ATP solution, more ATP was captured by the aptamer and more AuNPs/GO nanocomposites were removed from the modified electrode. As a result, energy transfer system was destroyed and the ECL intensity increased. It can be found from Figure 6D that the stable ECL intensity can be obtained when the aptasenor was incubated in ATP for 90 min. Therefore, 90 min was chosen as the optimal incubation time.

Analytical Performance of the Aptasensor for ATP Detection. Under the optimal conditions, the ECL intensities were recorded after the proposed aptasensors were incubated in different concentrations of ATP. It can be found from Figure 7 that the ECL intensity increased with the increase of ATP concentration because more aptamer was released from the modified electrode surface. As shown in the inset of Figure 7, a

DOI: 10.1021/acs.analchem.6b00921
Anal. Chem. 2016, 88, 5469−5475

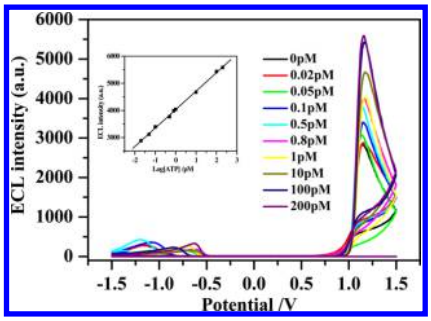

Figure 7. ECL curves of the aptasensor incubated in 0.02, 0.05, 0.1, 0.5, 0.8, 1, 10, 100, and 200 pM ATP. The inset is the calibration curve of ATP.

good linear relationship between the ECL intensity and the logarithmic value of ATP concentration can be obtained in the range of 0.02−200 pM. The standard calibration curve was I = 4055.9 + 684.6 log C_{ATP}, with a correlation coefficient of 0.9993. The detection limit was estimated to be 6.67 fM (S/N = 3), which was much lower than the previous reports as shown in Table S1.

The ECL emission from the ATP aptasensor incubated in 10 pM ATP was recorded under continuous potential scanning for nine cycles as shown in Figure 8A. The relative standard deviation (RSD) was less than 2.1%, indicating the good stability of the proposed aptasensor. The long-time stability of the aptasensor was investigated. When the aptasensor was stored at 4 °C, it retained at 92.4% of its initial response after a storage period of 2 weeks, indicating the proposed sensor had good long-term stability. The reproducibility of the aptasensor was examined on the same and on the different electrodes with the same ATP concentration. Relative standard deviation of five dependent measurements was less than 3.6% for the same electrode and less than 6.2% for five electrodes. Therefore, the ECL aptasensor has a relatively good reproduction in ATP detection.

The selectivity and the binding specificity of the proposed ECL aptasensor for ATP were evaluated. The contrast experiment was performed by measuring the changes of ECL intensity when the aptasensors were incubated in ATP and its analogues, such as cytidine triphosphate (CTP), guanosine triphosphate (GTP), and uridine triphosphate (UTP). It can be found from Figure 8B that the changes of ECL signal resulted from CTP, GTP, and UTP were less than 20% of that of ATP, even if their concentrations were 2000-fold higher than ATP. These results suggested that the present aptasensor had excellent selectivity for ATP.

Detection of ATP in Real Samples. The proposed ECL aptasensor was used to detect ATP in human serum samples. Because the concentration of human serum ATP is nearly 1000 nM level, the dilution of serum samples is necessary and 50 000-fold diluted serum was applied in the following experiment.[44] With a standard addition method, the amount of ATP in two human serum samples were detected to be 24 pM and 15 pM, respectively, which was similar to the result obtained with the reported method.[45] After the serum samples were spiked with 10 pM and 50 pM ATP, the recoveries for three detections were 94.5% ± 5.6% and 98.3% ± 4.5% for 10 pM ATP and 97.2% ± 5.9% and 93.8% ± 7.1% for 50 pM ATP, respectively, indicating acceptable accuracy. The results demonstrated that the ECL aptasensor can be used for quantification of ATP in real samples.

CONCLUSIONS

Strong anodic $Ru(bpy)_3^{2+}$ ECL has been obtained at the GO/GCE in the neutral condition without other coreactant. GO exhibited apparent electrocatalytical effect on the oxidation of $Ru(bpy)_3^{2+}$ and could act as the coreactant to generate ECL with $Ru(bpy)_3^{2+}$. A sandwich-like structure including GO film, ATP aptamer, and AuNPs/GO nanocomposites has been constructed via DNA hybridization. ECL-RET can occur between $Ru(bpy)_3^{2+}$ ECL and AuNPs/GO nanocomposites, resulting in the decreased ECL signal. The specificity bind between aptamer and target ATP could destroy the sandwich-like structure and AuNPs/GO nanocomposites could be released from the electrode. As a result, the ECL-RET was hampered and ECL signal increased linearly with ATP concentrations. The proposed ECL aptasensor exhibited good analytical performance and was successfully applied in real sample assays. Moreover, the energy transfer between $Ru(bpy)_3^{2+}$ ECL and AuNPs/GO nanocomposite provide a new avenue in the establishment of energy donor/acceptor pairs for ECL-RET investigation.

ASSOCIATED CONTENT

Supporting Information

The Supporting Information is available free of charge on the ACS Publications website at DOI: 10.1021/acs.analchem.6b00921.

Apparatus and additional experimental data (PDF)

AUTHOR INFORMATION

Corresponding Author

*E-mail: jjzhu@nju.edu.cn. Phone/fax: +86-25-89687204.

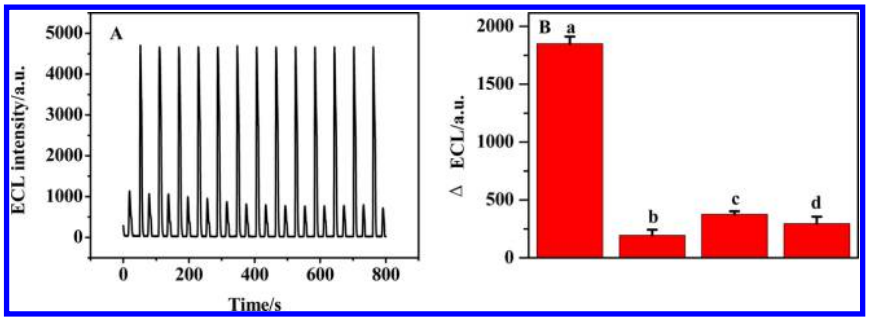

Figure 8. (A) Stability of the ECL immunosensor incubated in 10 pM ATP under consecutive cyclic potential scans for 13 cycles and (B) ECL variations of the aptasensor incubated in 10 pM ATP (a), 20 nM GTP (b), CTP (c), and UTP (d).

DOI: 10.1021/acs.analchem.6b00921
Anal. Chem. 2016, 88, 5469−5475

Notes

The authors declare no competing financial interest.

■ ACKNOWLEDGMENTS

This research was supported from National Natural Science Foundation of China (Grant Nos. 21335004, 21427807, and 21575002), Natural Science Foundation of Anhui Province (Grant No. 1408085MF114), Natural Science Foundation from the Bureau of Education of Anhui Province (Grant No. KJ2015A075), China Postdoctoral Science Foundation (Grant No. 2013M541637), and Jiangsu Province Postdoctoral Science Foundation (Grant No. 1302126C).

■ REFERENCES

(1) Richter, M. M. *Chem. Rev.* **2004**, *104*, 3003−3036.
(2) Miao, W. J.; Choi, J. P.; Bard, A. J. *J. Am. Chem. Soc.* **2002**, *124*, 14478−14485.
(3) Wang, H. J.; Yuan, R.; Chai, Y. Q.; Niu, H.; Cao, Y. L.; Liu, H. J. *Biosens. Bioelectron.* **2012**, *37*, 6−10.
(4) Yang, M. L.; Jiang, B. Y.; Xie, J. Q.; Xiang, Y.; Yuan, R.; Chai, Y. Q. *Talanta* **2014**, *125*, 45−50.
(5) Xiao, L. J.; Chai, Y. Q.; Yuan, R.; Cao, Y. L.; Wang, H. J.; Bai, L. J. *Talanta* **2013**, *115*, 577−582.
(6) Zhang, W. Z.; Zhang, J. M.; Zhang, H. L.; Cao, L. Y.; Zhang, R.; Ye, Z. Q.; Yuan, L. J. *Talanta* **2013**, *116*, 354−360.
(7) Yang, X. Y.; Wang, A. G.; Liu, J. L. *Talanta* **2013**, *114*, 5−10.
(8) Lin, Z. J.; Chen, X. M.; Jia, T. T.; Wang, X. D.; Xie, Z. X.; Oyama, M.; Chen, X. *Anal. Chem.* **2009**, *81*, 830−833.
(9) Shin, I. S.; Bae, S. W.; Kim, H.; Hong, J. I. *Anal. Chem.* **2010**, *82*, 8259−8265.
(10) Chi, Y. W.; Dong, Y. Q.; Chen, G. N. *Anal. Chem.* **2007**, *79*, 4521−4528.
(11) Rubinstein, I.; Bard, A. J. *J. Am. Chem. Soc.* **1980**, *102*, 6641−6642.
(12) Chen, X.; Sato, M. *Anal. Sci.* **1995**, *11*, 749−754.
(13) Zorzi, M.; Pastore, P.; Magno, F. *Anal. Chem.* **2000**, *72*, 4934−4939.
(14) Choi, H. N.; Cho, S. H.; Lee, W. Y. *Anal. Chem.* **2003**, *75*, 4250−4256.
(15) Chow, K. F.; Mavre, F.; Crooks, J. A.; Chang, B. Y.; Crooks, R. M. *J. Am. Chem. Soc.* **2009**, *131*, 8364−8365.
(16) Shi, L. F.; De Paoli, V.; Rosenzweig, N.; Rosenzweig, Z. *J. Am. Chem. Soc.* **2006**, *128*, 10378−10379.
(17) Clapp, A. R.; Medintz, I. L.; Mauro, J. M.; Fisher, B. R.; Bawendi, M. G.; Mattoussi, H. *J. Am. Chem. Soc.* **2004**, *126*, 301−310.
(18) Huang, X. Y.; Li, L.; Qian, H. F.; Dong, C. Q.; Ren, J. C. *Angew. Chem.* **2006**, *118*, 5264−5267.
(19) Zhao, S. L.; Huang, Y.; Liu, R. J.; Shi, M.; Liu, Y. M. *Chem. - Eur. J.* **2010**, *16*, 6142−6145.
(20) Yao, H. Q.; Zhang, Y.; Xiao, F.; Xia, Z. Y.; Rao, J. H. *Angew. Chem., Int. Ed.* **2007**, *46*, 4346−4349.
(21) Li, L. L.; Chen, Y.; Lu, Q.; Ji, J.; Shen, Y. Y.; Xu, M.; Fei, R.; Yang, G. H.; Zhang, K.; Zhang, J. R.; Zhu, J. J. *Sci. Rep.* **2013**, *3*, 1529.
(22) Li, Y. J.; Gao, W.; Ci, L. J.; Wang, C. M.; Ajayan, P. M. *Carbon* **2010**, *48*, 1124−1130.
(23) Kuila, T.; Bose, S.; Khanra, P.; Mishra, A. K.; Kim, N. H.; Lee, J. H. *Biosens. Bioelectron.* **2011**, *26*, 4637−4648.
(24) Yan, Z.; Li, Y.; Zheng, J. B.; Zhou, M. *J. Electroanal. Chem.* **2014**, *731*, 133−138.
(25) Liu, P. Z.; Hu, X. W.; Mao, C. J.; Niu, H. L.; Song, J. M.; Jin, B. K.; Zhang, S. Y. *Electrochim. Acta* **2013**, *113*, 176−180.
(26) Liu, F.; Choi, J. Y.; Seo, T. S. *Biosens. Bioelectron.* **2010**, *25*, 2361−2365.
(27) Ping, J. F.; Zhou, Y. B.; Wu, Y. Y.; Papper, V.; Boujday, S.; Marks, R. S.; Steele, T. W. J. *Biosens. Bioelectron.* **2015**, *64*, 373−385.
(28) Eda, G.; Lin, Y. Y.; Mattevi, C.; Yamaguchi, H.; Chen, H. A.; Chen, I. S.; Chen, C. W.; Chhowalla, M. *Adv. Mater.* **2010**, *22*, 505−509.
(29) Subrahmanyam, K. S.; Kumar, P.; Nag, A.; Rao, C. N. R. *Solid State Commun.* **2010**, *150*, 1774−1777.
(30) Loh, K. P.; Bao, Q.; Eda, G.; Chhowalla, M. *Nat. Chem.* **2010**, *2*, 1015−1024.
(31) He, Y.; Huang, G. M.; Jiang, J.; Zhang, Q.; Cui, H. *Carbon* **2013**, *56*, 201−207.
(32) Jung, J. H.; Cheon, D. S.; Liu, F.; Lee, K. B.; Seo, T. S. *Angew. Chem., Int. Ed.* **2010**, *49*, 5708−5711.
(33) Zeng, X. X.; Ma, S. S.; Bao, J. C.; Tu, W. W.; Dai, Z. H. *Anal. Chem.* **2013**, *85*, 11720−11724.
(34) Jana, N. R.; Gearheart, L.; Murphy, C. J. *Langmuir* **2001**, *17*, 6782−6786.
(35) Kovtyukhova, N. I.; Ollivier, P. J.; Martin, B. R.; Mallouk, T. E.; Chizhik, S. A.; Buzaneva, E. V.; Gorchinskiy, A. D. *Chem. Mater.* **1999**, *11*, 771−778.
(36) Xiong, Y.; Deng, C. H.; Zhang, X. M. *Talanta* **2014**, *129*, 282−289.
(37) Guo, S. J.; Sun, S. H. *J. Am. Chem. Soc.* **2012**, *134*, 2492−2495.
(38) Dong, Y. P.; Zhang, J.; Ding, Y.; Chu, X. F.; Zhang, W. B. *J. Electrochem. Soc.* **2012**, *159*, H692−H696.
(39) Yuan, Y. L.; Li, H. J.; Han, S.; Hu, L. Z.; Parveen, S.; Cai, H. R.; Xu, G. B. *Anal. Chim. Acta* **2012**, *720*, 38−42.
(40) Zu, Y. B.; Bard, A. J. *Anal. Chem.* **2000**, *72*, 3223−3232.
(41) Shan, C. S.; Yang, H. F.; Han, D. X.; Zhang, Q. X.; Ivaska, A.; Niu, L. *Biosens. Bioelectron.* **2010**, *25*, 1070−1074.
(42) Yuan, Y. L.; Han, S.; Hu, L. Z.; Parveen, S.; Xu, G. B. *Electrochim. Acta* **2012**, *82*, 484−492.
(43) Jin, Y. H.; Huang, S.; Zhang, M.; Jia, M. Q.; Hu, D. *Appl. Surf. Sci.* **2013**, *268*, 541−546.
(44) Liu, J. H.; Wang, C. Y.; Jiang, Y.; Hu, Y. P.; Li, J. S.; Yang, S.; Li, Y. H.; Yang, R. H.; Tan, W. H.; Huang, C. Z. *Anal. Chem.* **2013**, *85*, 1424−1430.
(45) Liu, Y. T.; Lei, J. P.; Huang, Y.; Ju, H. X. *Anal. Chem.* **2014**, *86*, 8735−8741.

DOI: 10.1021/acs.analchem.6b00921
Anal. Chem. 2016, 88, 5469−5475